



**HAL**  
open science

## Mining spectral libraries to study sensors' discrimination ability

Germain Forestier, Jordi Inglada, Cédric Wemmert, Pierre Gancarski

► **To cite this version:**

Germain Forestier, Jordi Inglada, Cédric Wemmert, Pierre Gancarski. Mining spectral libraries to study sensors' discrimination ability. SPIE Europe Remote Sensing, Aug 2009, Berlin, Germany. 10.1117/12.830392 . hal-01887503

**HAL Id: hal-01887503**

**<https://hal.science/hal-01887503>**

Submitted on 4 Oct 2018

**HAL** is a multi-disciplinary open access archive for the deposit and dissemination of scientific research documents, whether they are published or not. The documents may come from teaching and research institutions in France or abroad, or from public or private research centers.

L'archive ouverte pluridisciplinaire **HAL**, est destinée au dépôt et à la diffusion de documents scientifiques de niveau recherche, publiés ou non, émanant des établissements d'enseignement et de recherche français ou étrangers, des laboratoires publics ou privés.

# Mining spectral libraries to study sensors' discrimination ability

Germain Forestier<sup>1</sup> and Jordi Inglada<sup>2</sup> and Cedric Wemmert<sup>1</sup> and Pierre Gancarski<sup>1</sup>

<sup>1</sup>University of Strasbourg, LSIIT, 67412 Illkirch, France;

<sup>2</sup>Centre National d'Etudes Spatiales, 31401 Toulouse, France

## ABSTRACT

In remote sensing data classification, the ability to discriminate different land cover or material types is directly linked with the spectral resolution and sampling provided by the optical sensor.<sup>1</sup> Several previous studies<sup>2-4</sup> showed that the spectral resolution is a critical issue, especially to discriminate different land covers in urban areas. In spite of the increasing availability of hyperspectral data, multispectral optical sensors on board of several satellites are still acquiring everyday a massive amount of data with a relatively poor spectral resolution (i.e. usually about 4 to 7 spectral bands). These remotely sensed data are intensively used for Earth observation regardless of their limited spectral resolution.

In this paper, we propose to study the capacity of discrimination of several of these optical sensors : Pleiades, QuickBird, SPOT5, Ikonos, Landsat TM, Formosat and Meris. To achieve this goal, we used different spectral libraries which provide spectra of materials and land covers generally with a fine spectral resolution. These spectra were extracted from these libraries and convolved with the Relative Spectral Responses (RSR) of each sensor to create spectra at the sensors' resolutions. Then, these reduced spectra were evaluated thanks to a classical separability index and machine learning tools. This study focuses on the capacity of each sensor to discriminate different materials according to its spectral resolution. As the spectra for each sensor are created from the exact same spectra extracted from the libraries, the only variation is the RSR of the sensors. This approach allows us to fairly compare the different ability of the sensors to discriminate materials.

## 1. INTRODUCTION

The spectral resolution of a sensor can be characterized by the number of spectral bands, their bandwidths and their locations along the spectrum<sup>3</sup>. Spectral resolution is also described by Lillesand and Kiefer<sup>5</sup> as "the ability to discriminate fine spectral differences". Several previous studies<sup>2-4</sup> showed that the spectral resolution is a critical issue, especially to discriminate different land covers in complex environment like urban areas. Most of multispectral systems have 4 to 7 spectral bands within the visible to middle infrared region of the electromagnetic spectrum.<sup>6</sup> There exist however some systems that use one or more thermal infrared bands. One of the main advantages compared to hyperspectral acquisition, is the larger spatial coverage, which allows a faster and wider mapping of large areas. Indeed, satellite remote sensing systems provide both, a synoptic view space and economies of scale<sup>6</sup>.

In this study, we used different spectral libraries, which provide spectra of materials and land covers with a fine spectral resolution. These spectra were extracted from these libraries and convolved with the Relative Spectral Responses (RSR) of several sensors to create spectra at the sensors' resolutions. This study focuses on the capacity of each sensor to discriminate different materials, according to its spectral resolution. As the spectra for each sensor are created from exactly the same spectra extracted from the libraries, the only variation is the RSR of the sensors.

---

Further author information: (Send correspondence to Germain Forestier)

Germain Forestier: E-mail: forestier@unistra.fr

## 2. SENSOR SIMULATION

### 2.1 Previous work

Sensor simulation, also called band simulation or band synthesis, consists in generating simulated multispectral spectra from data acquired by existing sensors, with higher spectral resolution. This simulation consists in combining narrow hyperspectral bands into broader multispectral bands. This kind of approach has already been used, especially for sensor calibration and sensor simulation. The spectra simulation step uses the Relative Spectral Response (RSR) functions of the multispectral sensor, which describes the spectral response of each simulated sensor's band.

Green et al.<sup>7</sup> used band synthesis for cross-calibration of a satellite multispectral instrument using AVIRIS data. The simulated data were used to determine the on-orbit radiometric calibration coefficients required for calibration of the spectral bands of the satellite. A similar approach was used by Chander et al.<sup>8</sup> for the cross-calibration of the Advanced Land Imager (ALI) from Landsat ETM+ well-calibrated data. Salvatore et al.<sup>9</sup> used band simulation to simulate the response of a new sensor from AVIRIS data. This simulation allowed the investigators to evaluate in advance the potentialities of the new multispectral sensor. This kind of simulation provides an opportunity to try variations in the original spectral response, and to adjust the RSR to achieve better results for the multispectral sensor objectives. Jarecke et al.<sup>10</sup> used Hyperion hyperspectral data to simulate Landsat ETM+ data and evaluated that the difference between the simulated data and real data actually acquired by Landsat ETM+ was around 10%. Meyer et al.<sup>2</sup> used AVIRIS data to simulate MODIS and Landsat ETM+ data in order to illustrate how the differences in the RSR affect the observation of some typical surface features. The authors noticed some strong variations according to the different RSR. They concluded that more investigations were needed on how RSR affects the observation of different surfaces. Franke et al.<sup>11</sup> used band simulation to compare the differences of Normalized Difference Vegetation Index (NDVI) according to the RSR of Landsat TM, Quickbird and SPOT5. The assessment of NDVI differences showed substantial variations between sensor systems. An intercalibration approach to adjust NDVI difference caused by varying RSR functions using a polynomial order is suggested. Kruse et al.,<sup>12</sup> used the simulation to combine hyperspectral and multispectral images. Hyperspectral data were used to extract endmembers, which were then simulated at multispectral resolution. These endmembers were then used to extend the hyperspectral mapping to the larger spatial coverage offered by the multispectral data. Herold et al.<sup>3</sup> studied spectral resolution requirements for mapping urban areas. They used AVIRIS data and an urban spectral library to study the most suitable spectral bands in separating urban land cover types. The AVIRIS data were also used to simulate Landsat TM and Ikonos data. The results showed that Ikonos and Landsat TM lack of spectral details to efficiently map several urban classes.

#### 2.1.1 Sensor simulation method

To simulate multispectral data from hyperspectral data, the responses of narrow hyperspectral bands have to be aggregated. However, the reflectance values of the hyperspectral narrow bands cannot be summed directly to reproduce multispectral bands. Indeed, they must be weighted to account for the relative response of the multispectral bands. The RSR of each band of a sensor system is characterized by the effective spectral quantum efficiency, which indicates the spectral sensitivity of the band at each wavelength<sup>11</sup>. Each sensor has consequently a different spectral sensitivity, which is described by its individual RSR functions. Figure 1 shows three examples of RSR functions for Quickbird, SPOT5 and Landsat ETM.

As stated by Clark et al.<sup>13</sup>, different strategies have been proposed to compute the weights to apply to each hyperspectral band. For the simulation used in this paper, each hyperspectral center wavelength was linked with the mean RSR value (in the range of the *full width half maximum* (FWHM) of the hyperspectral spectral band) of the simulated band. This approach is similar to the one proposed by Franke et al.<sup>11</sup>.

One should notice that in this study some external parameters are not simulated. For example, some other simulation approaches<sup>14</sup> take into account other variables like atmospheric effects or geometric differences between sensors. In this study, we are interested on the sensor discrimination ability according to their RSR, that is why we only focused on spectral difference caused by different RSR functions. However other aspects like the spatial resolution should also be investigated and simulated to truly assess the difference between sensors. However, focusing only on spectral resolution already provides some insight on the different sensors ability.

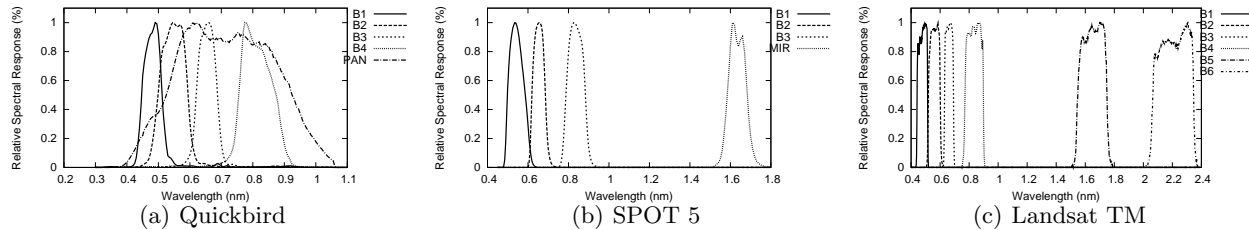


Figure 1. Example of three Relative Spectral Response (RSR).

### 3. SPECTRAL LIBRARIES

#### 3.1 Available spectral libraries

The advent of spectroscopy and remote sensing has offered an opportunity to develop a new kind of stored knowledge through spectral libraries. These spectral libraries are repository of spectra of various kinds of materials (e.g. mineral, man-made material, vegetation...) generally captured *in situ* using field instruments. Everybody agrees on the importance of the challenging problem to create such libraries in order to store, share and reuse information about materials. However, the number of these libraries freely available and easily accessible is relatively limited. Indeed, an important number of factors limits their development, starting by the cost of field acquisitions and the time needed to structure and organize the spectra in a meaningful way. In this section, we review the major available spectral libraries and their characteristics.

The most common and probably the most widely used library is the ASTER spectral library<sup>15</sup>. This library includes contributions from the Jet Propulsion Laboratory (JPL), Johns Hopkins University (JHU) and the United States Geological Survey (USGS). The library includes spectra of rocks, minerals, lunar soils, terrestrial soils, man-made materials, meteorites, vegetation, snow and ice covering the visible through thermal infrared wavelength region (0.4-15.4  $\mu\text{m}$ ). The first version was released in July 1998 and the second one is available since 2007 on simple request through the library website\*. The USGS also offers its own library<sup>16</sup> which is freely available for download †. Researchers at the USGS Spectroscopy Lab have measured the spectral reflectance of hundreds of materials in the lab and have compiled a spectral library. This library contains over 1300 spectra organized in six groups: minerals, soils, coatings, liquid, man-made and plants. To the best of our knowledge these two libraries (ASTER and USGS) are the most comprehensive and freely available libraries. Other smaller projects provide sometimes spectra, as for example the National Center for Geographic Information and Analysis (NCGIA) which offers a small spectral library of urban spectra. The spectral library developed for this project contains over 130 averaged spectra from AVIRIS sensor structured in 7 urban classes. The library is available for download on the project website‡. Herold et al.<sup>1</sup> also created a library of more than 4500 individual urban spectra from the city of Santa Barbara categorized in 108 unique surface types. Another library of 270 spectra from AVIRIS data was also developed.

Several attempts to create platforms to store and to share spectra also exist. For example, Hueni et al.<sup>17</sup> proposed a software named SPECCHIO<sup>§</sup>, which is a tool to hold and structure reference spectra using a database. The authors make the distinction between spectral library (i.e. spectra list) and spectral database (i.e structured spectra with metadata). An interesting reflexion is carried out on the need to use standards and metadata. Ferwana et al.<sup>18</sup> also offer a similar system through a website ¶ where researchers can store and share their spectra. The German aerospace center (DRL) also provides a spectral archive website || with the intention to create a universal tool for archiving, managing and using spectra collected from various projects. Although these

\*<http://speclib.jpl.nasa.gov>

†<http://speclab.cr.usgs.gov>

‡<http://ncgia.ucsb.edu>

§<http://www.specchio.ch>

¶<http://www.hyperspectral.info>

|| <http://www.cocoon.caf.dlr.de>

attempts to offer ways to share and store spectra are very interesting, they generally offer tools to structure spectra but only provide few spectra. Furthermore, the multiplication of these tools tends to bring confusion to the user interested in creating and managing a spectral library. It is worth noticing that all these different libraries are structured following their own format, which increases the difficulty to gather information coming from various sources.

In this study, four different libraries were used to assess the discrimination ability of the different sensors. Table 1 summarizes the specifications of the different libraries.

Nom	# Classes	# Spectra	# Leves	Instrument	Wavelegnth range
ASTER/JHU	3/5/12	270	3	Beckman/Nicolet	[0.4;14.0] $\mu\text{m}$
USGS	4	860	1	Beckman/ASD/Nicolet	[0.35;2.5] $\mu\text{m}$
NCGIA	7	133	1	AVIRIS	[0.37;2.5] $\mu\text{m}$
HEROLD	4/8/19/26	956	4	AVIRIS	[0.37;2.5] $\mu\text{m}$

Table 1. Spectral libraries available.

## 4. EVALUATION

### 4.1 Class separability evaluation

Separability criteria<sup>19</sup> aim at evaluating the separability of the classes of a dataset in a given feature space. Different criteria have been proposed in the literature to evaluate and quantify this separability. For remote sensing applications, the divergence criterion (D), the transformed divergence criterion (TD), the Bhattacharyya distance (B) and the Jeffreys-Matusita distance (JM) are the most widespread criteria. These criteria have been mainly used in feature selection problems, where the goal is to select the best subset of 'informative' or 'relevant' features for a given dataset, in order to maximize classification accuracy for this reduced number of features. In multispectral and hyperspectral image classification, these criteria were used to select the best subset of bands<sup>20-22</sup>. Indeed, some bands may be noisy or correlated, and consequently provide a misleading information about class separability. Ranson et al.<sup>23</sup> also used the JM distance to compare the separability of the same thematic classes in two different images, an optical one and a radar one. This study was carried out to choose which image was the most suited to identify these classes. Assuming a Gaussian distribution, these criteria use the mean and the covariance matrix of the classes.

The choice between Jeffreys-Matusita distance and the divergence to evaluate the separability of a set of classes is not trivial. Richards and Jia<sup>24</sup> claim that Jeffreys-Matusita distance tends to perform better as a feature selection criterion than the divergence, but is computationally more complex. This is mainly due to the high number of matrix operations required to compute the Bhattacharyya distance. The Jeffreys-Matusita distance and the transformed divergence are described as almost as effective and considerably better than simple divergence and simple Bhattacharyya, essentially thanks to their bounded range. The Jeffreys-Matusita distance and the transformed divergence seem equally used in the literature without clear arguments on why choosing one or the other. In this paper we chose to use the Jeffreys-Matusita distance.

### 4.2 Classification accuracy

#### 4.2.1 Motivation of the evaluation

Another way to evaluate class separability and to assess features relevance is to perform a supervised classification of the dataset. The accuracy and the confusion matrix of the classification are useful tools to assess the quality of features. Indeed, as stated by Uta et al.<sup>4</sup>, separability criteria can suffer from some problems in extreme cases. For example, a class can show a good separability with the other classes with a constant overlap of 5% for each class in the feature space. However, the total spectral overlap can range from 5% allowing a classification of good quality to 100% making the accurate classification of this material impossible. Furthermore, the computation of the Bhattacharyya distance requires the calculation of the inverse of the covariance matrix, which can be sometimes problematic. Indeed, when the number of features increases, the covariance matrix tends to become singular and consequently not invertible.

### 4.2.2 Configuration of the evaluation

To evaluate the classification performance on the spectral libraries we used an ensemble classifier system<sup>25</sup>, which combines three different supervised methods: a 1-Nearest-Neighbour classifier, a Naive Bayes classifier, and a C4.5 classifier. These classifiers were combined through a majority voting strategy. This choice has been made to reduce the bias involved in the selection of a single algorithm. For the experiment, 10-cross-validation has been used. It consists in splitting the dataset in 10 subsets and then, in learning on  $\frac{9}{10}$  of the dataset and then evaluating on the remaining  $\frac{1}{10}$ . The evaluation is computed for all the combinations. This approach avoids to split the dataset in a learning set and an evaluation set and is statistically more relevant (as each sample is used alternatively for learning and testing).

## 5. EXPERIMENTS

### 5.1 Presentation

In this section, we present three different experiments carried out to illustrate the usefulness of sensor simulation. In the first experiment (Section 5.3), we compared the different sensors according to their spectral response defined by their RSR function. The different libraries presented in Section 3 were convolved with the RSR of each sensor. Then, separability index and classification accuracy were computed in order to compare the different sensors. Hence, we were able to gain some insight on the sensor ability to classify materials accurately. Furthermore, the comparison is fair as the dataset for each sensor is created from the exact same spectral libraries. The only variation for each dataset is the RSR used to convolve the spectra.

The second experiment (Section 5.4), consisted in evaluating the potential interest of spectral indexes (e.g., NDVI). The aim of this simulation was to evaluate if a specific spectral index is useful for the classification of a specific material, and if the sensors were able to leverage this new information. Classification accuracy assessment and separability evaluation were conducted with and without the use of spectral indexes in order to evaluate the interest of their addition to the dataset.

The last experiment (Section 5.5) illustrates one of the many potential use of sensor simulation. In this experiment we evaluated the interest of a specific band, namely the Short-Wave Infra-Red band (SWIR). To study the usefulness of this band we carried out two evaluations: the first one consisted in removing the SWIR band from a sensor equipped of this band, when the second one consisted in adding this band to a sensor not originally equipped. This experiment reveals how sensor simulation can be used to design new sensor and evaluate the interest of a specific spectral band.

### 5.2 Sensors list

Different sensors were used during the experiments. Table 2 summarizes the information about them. We used some of the most common multispectral systems available.

Name	# Bands	# Owner
Spot 5	4	CNES
Quickbird	5	Digital Globe
Pleiades	5	CNES
Landsat TM	6	NASA
Ikonos	4	Satellite Imaging Corporation
Formosat	5	Taiwan
Meris	15	ESA

Table 2. Simulated sensors list.

### 5.3 Sensors evaluation and comparison

In this first experiment the different libraries were used to compare the different sensors. The results are presented in Table 3 and are detailed for each dataset hereafter. The accuracy of the ensemble classifier is presented in the column Vote, and the Jeffreys-Matusita distance in the column JM.

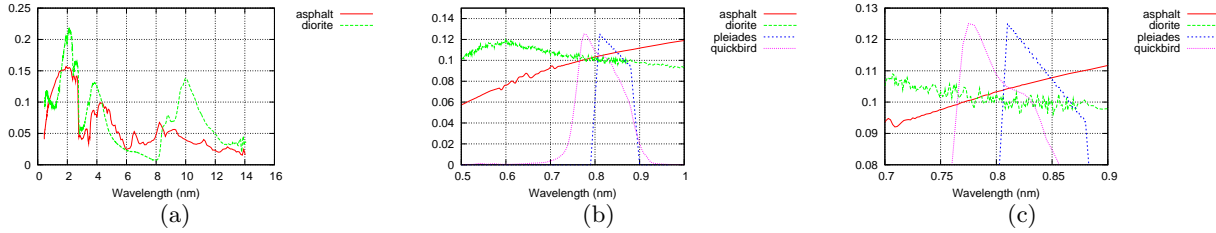


Figure 2. Asphalt (Man-Made), Diorite (Rocks) (a) and the NIR bands of Quickbird and Pleiades (c)

### 5.3.1 ASTER

For this dataset, the Ikonos and Formosat sensors give the worst results. This is consistent as they have a low spectral resolution compared to the other studied sensors. They are followed by Spot 5, Quickbird and Pleiades and finally Meris which achieves the best results. An interesting point to notice in these results is the relative large difference between the accuracy of Quickbird (84.4%) and Pleiades (92.2%). As these two sensors have the same number of bands which are very similar, one could expect a similar behaviour in classification accuracy. However, even if the RSR are strongly similar, there are still some small variations. The most important difference in the bands of these two sensors is the Near Infra Red (NIR) band. To check if the difference of accuracy was due to this difference of RSR, we removed the NIR band of these two sensors and ran the classification again. This time, the accuracies were quite close with 83.3% for Pleiades and 81.5% for Quickbird. Then, we replaced the NIR band of Quickbird by the NIR band of Pleiades to check if the NIR band of Pleiades was truly responsible of the higher accuracy. We obtained this time 92.2% for Pleiades and 91.1% for Quickbird (instead of 84.4% with its own NIR band). These results supported our hypothesis that the variation in the NIR band was responsible of the difference of accuracy.

We investigated more closely the results to identify some examples where Pleiades was able to correctly discriminate two specific spectra, whereas Quickbird was not. We identified several couples of spectra misclassified by Quickbird and well classified by Pleiades. We present here two examples, one couple of Asphalt (Man-Made) and Diorite (Rocks) (see Figure 2), and one couple of Asphalt (Man-Made) and Basalt (Rocks) (see Figure 3). In these two set of figures, one can see that the NIR bands of the two sensors are quite similar, but not exactly defined in the same range of wavelengths. This small shift on the wavelength seems to be responsible of the difference of accuracy. On Figure 2 and Figure 3, one can clearly see that the two spectra are very confused in the range of the Quickbird NIR band while they seem to be more separable in the Pleiades NIR band range.

These results are consistent with previous studies which also pointed out that even small variations in band definition can imply differences in spectral response of some materials. For example, Franke et al.<sup>11</sup> showed that the variation on the NIR band of different sensors leads to strong variation in the calculation of the NDVI. Meyer et al.<sup>2</sup> also showed that the definition of the RSR is a key issue to allow the identification of some type of materials.

The conclusion that can be drawn from these results is not that Pleiades is better than Quickbird, but rather than even two sensors having similar bands can produce different results according to the application. Furthermore, these differences might be estimated and evaluated thanks to sensors simulation as presented in this study.

### 5.3.2 USGS

The results for the USGS dataset are consistent with the spectral resolution of the sensors. The best results are achieved by Landsat and Meris with an accuracy of 79.5%. It seems that the Landsat bands are especially well suited for this dataset and helps to better discriminate several spectra confused by the other sensors.

### 5.3.3 NCGIA

The best results for this dataset are achieved by Spot 5 sensor. The Middle Infra Red (MIR) channel seems useful in this application to discriminate some urban land covers like *Road* and *Roof*, which are well known as difficult to classify.

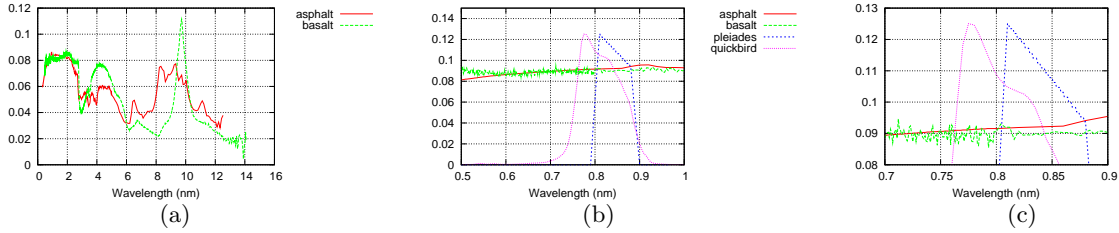


Figure 3. Asphalt (Man-Made), Basalt (Rocks) (a) and the NIR bands of Quickbird and Pleiades (b) (c)

	Ikonos		Pleiades		Quickbird		Formosat		Landsat TM		Spot5		Meris	
	JM	Vote	JM	Vote	JM	Vote	JM	Vote	JM	Vote	JM	Vote	JM	Vote
Aster I	0,79	83,33	0,82	92,22	0,76	84,44	0,76	84,81	0,85	94,44	0,76	89,25	0,92	94,44
Aster II	1,20	53,33	1,21	61,11	1,23	51,48	1,16	51,11	1,29	62,59	1,16	57,77	1,55	64,81
Aster III	1,31	45,18	1,29	50,00	1,31	44,81	1,28	45,92	1,33	48,88	1,26	50,74	1,60	51,85
NCGIA	1,38	59,39	1,38	62,40	1,39	61,65	1,38	60,15	1,41	60,90	1,37	63,15	0,76	56,81
USGS	0,84	77,09	0,86	77,66	0,84	75,93	0,84	76,49	0,92	79,53	0,86	77,54	1,21	79,52
Herold I	0,79	96,44	0,78	96,54	0,78	96,44	0,78	96,86	0,81	97,80	0,78	96,75	0,75	97,28
Herold II	1,28	91,52	1,26	91,84	1,30	90,58	1,23	91,73	1,31	93,30	1,29	91,63	0,89	92,25
Herold III	1,76	85,66	1,74	86,61	1,76	85,14	1,75	85,35	1,80	91,42	1,78	88,18	1,55	88,38
Herold IV	1,84	85,35	1,81	86,71	1,84	85,25	1,82	85,14	1,85	90,69	1,84	88,38	1,75	87,44

Table 3. Influence of the NDVI

### 5.3.4 Herold

One of the interesting feature of this dataset is the organisation of the class on four levels. Consequently, it is interesting to study the behaviour of the sensors according to the level of classification. Indeed, the classification task is expected to be more difficult as the number of classes increases, as the probability of confusion between the classes increases as well. In level I and II the results are barely similar among the different sensors with an accuracy around 96% for level I and 91% for level II. However, at level III, some differences of accuracy appear and again, the sensor with better spectral resolution have better results. Landsat has particularly good results with an accuracy of 91.4% followed by Meris with 88.3%. The trend is maintained on level IV. This kind of experiment allows us to gain some insight on the capacity of the sensors to map land cover at certain levels. If a user is interested in mapping some general classes (Level I and II), the choice of the sensor is not crucial. However, if the user is interested in mapping specific classes deeper in the hierarchy (Level III and IV), the user should carefully select a sensor which accurately maps these classes.

## 5.4 Spectral index assessment

Simulation can also be used to estimate the interest of a spectral index for classification. Spectral indexes are non linear combinations of bands which are used to highlight some specific features in images (vegetation, soil, buildings, water ...). Simulation can be used to evaluate is the addition of a spectral index improves the separability of the classes along with the classification accuracy. We give in this section a simple example with the famous NDVI. We classified the dataset generated for Ikonos, Pleiades, Quickbird and Spot 5 with and without the addition of the NDVI.

The results presented in Table 4 reveal that the addition of the NDVI tends to increase the classification accuracy for most of the datasets but not for all (e.g. NCGIA). In this experiment, Spot 5 does not seem to leverage the information provided by the NDVI, except for the Herold dataset where the NDVI seems informative for all the sensors. This kind of simulation might be used with more indexes to evaluate their usefulness.

## 5.5 Further simulations

In this section, we present another type of simulation also available with this kind of approach. For example, simulation can be used to evaluate if the addition of a band to a sensor is relevant for a certain type of application. To illustrate this, we choose to evaluate how the Pleiades sensor reacts to the addition of the Short-Wave Infra

	Ikonos		Pleiades		Quickbird		Spot5	
	D	D+NDVI	D	D+NDVI	D	D+NDVI	D	D+NDVI
Aster I	83,33	83,70 ●	92,22	93,70 ●	84,44	84,07 ○	89,25	87,03 ○
Aster II	53,33	54,44 ●	61,11	61,85 ●	51,48	55,92 ●	57,77	56,66 ○
Aster III	45,18	45,55 ●	50,00	51,85 ●	44,81	45,18 ●	50,74	44,07 ○
NCGIA	59,39	60,90 ●	62,40	57,89 ○	61,65	60,15 ○	63,15	60,15 ○
USGS	77,09	76,86 ○	77,66	79,06 ●	75,93	76,74 ●	77,54	78,36 ●
Herold I	96,44	97,49 ●	96,54	97,38 ●	96,44	97,80 ●	96,75	96,96 ●
Herold II	91,52	92,36 ●	91,84	91,21 ○	90,58	91,52 ●	91,63	92,25 ●
Herold III	85,66	88,91 ●	86,61	88,38 ●	85,14	87,97 ●	88,18	88,28 ●
Herold IV	85,35	87,86 ●	86,71	88,91 ●	85,25	88,59 ●	88,38	88,59 ●

Table 4. Influence of the NDVI

Red band (SWIR) and how the Spot 5 sensor reacts to its removal. The results are presented in Table 5. One can see that the addition of the SWIR band to Pleiades sensor does not seem to improve the results in this specific experiment. However its removal to the Spot 5 sensor greatly influences the classification results as the accuracy are always lower without this band.

	Pleiades		Spot5	
	D	D+MIR	D	D-MIR
Aster I	92,22	88,88 ○	89,25	87,77 ○
Aster II	61,11	62,96 ●	57,77	55,55 ○
Aster III	50,00	49,63 ○	50,74	48,88 ○
NCGIA	62,40	62,40 ○	63,15	57,14 ○
USGS	77,66	78,24 ●	77,54	75,32 ○
Herold I	96,54	96,96 ●	96,75	95,81 ○
Herold II	91,84	92,99 ●	91,63	90,79 ○
Herold III	86,61	88,59 ●	88,18	83,05 ○
Herold IV	86,71	89,12 ●	88,38	84,62 ○

Table 5. Influence of the MIR channel

## 6. CONCLUSION

In this study, we presented how sensor simulation can be used to evaluate the ability of a sensor to discriminate materials. This approach allows the user to compare different sensors on a specific application, but also to gain some insights on the potential of a sensor. However, the results presented in this study have to be balanced by the relative low number of spectra present in the available data set and their relevance for different applications. Indeed, spectral libraries are expensive to develop and consequently they are rarely distributed freely.

The tedious process of sensor design could be greatly backed by early simulation which could help to design specific RSR. This kind of simulation is still an unexplored wilderness and possesses a great potential for various applications. However, it is worth noticing that the simulation in this study did not take into account a certain number of important factors like the atmosphere, the spatial resolution of the sensor, the mixture of spectra, etc. Further work is necessary to improve the simulation task to take into account more parameters and consequently to be closer to the reality.

## Acknowledgment

The authors would like to thank the several authors contacted about their work on band simulation, especially Olivier Hagolle and Vanessa Heinzl for providing some RSR functions, Martin Herold for providing the spectral library, Taskin Kavzoglu and Mark Cutler for providing their results.

## REFERENCES

- [1] Herold, M., Roberts, D. A., Gardner, M. E., and Dennison, P. E., "Spectrometry for urban area remote sensing : Development and analysis of a spectral library from 350 to 2400 nm," *Remote Sensing of Environment* **91**, 304–319 (2004).

- [2] Meyer, D. and Chander, G., "The effect of variations in relative spectral response on the retrieval of land surface parameters from multiple sources of remotely sensed imagery," *IEEE International Geoscience and Remote Sensing Symposium*, 5150–5153 (2007).
- [3] Herold, M., Gardner, M., and Roberts, D., "Spectral resolution requirements for mapping urban areas," *IEEE Transactions on Geoscience and Remote Sensing* **41**(9), 1907–1919 (2003).
- [4] Heidena, U., Segl, K., Roessner, S., and Kaufmann, H., "Determination of robust spectral features for identification of urban surface materials in hyperspectral remote sensing data," *Remote Sensing of Environment* **111**, 537–552 (2007).
- [5] Lillesand, T. M. and Kiefer, R. W., [*Remote Sensing and Image Interpretation*], John Wiley & Sons (1994).
- [6] Govender, M., Chetty, K., and Bulcock, H., "A review of hyperspectral remote sensing and its application in vegetation and water resource studies," *Water SA* **33**(2), 145–152 (2007).
- [7] Green, R. O. and Shimada, M., "On-orbit calibration of a multi-spectral satellite sensor using a high altitude airborne imaging spectrometer," *Advances in Space Research* **19**, 1387–1398 (1997).
- [8] Chander, G., Meyer, D., and Helder, D., "Cross calibration of the landsat-7 etm+ and eo-1 ali sensor," *IEEE Transactions on Geoscience and Remote Sensing* **42**(12), 2821–2831 (2004).
- [9] Salvatore, E., Esposito, C., Krug, T., and Green, R., "Simulation of the spectral bands of the ccd and wfi cameras of the cbers satellite using aviris data," (1999).
- [10] Jarecke, P., Barry, P., Pearlman, J., and Markham, B., "Aggregation of hyperion hyperspectral spectral bands into landsat-7 etm+ spectral bands," *IEEE International Geoscience and Remote Sensing Symposium* **6**, 2822–2824 (2001).
- [11] Franke, J., Heinzl, V., and Menz, G., "Assessment of ndvi- differences caused by sensor specific relative spectral response functions," *IEEE International Geoscience and Remote Sensing Symposium*, 1138–1141 (2006).
- [12] Kruse, F. A., "Improving multispectral mapping by spectral modeling with hyperspectral signatures," *Journal of Applied Remote Sensing* **3** (2009).
- [13] Clark, R. N., Swayze, G. A., Livo, K. E., Kokaly, R. F., King, T. V. V., Dalton, J. B., Vance, J. S., Rockwell, B. W., Hoefen, T., and McDougal, R. R., "Synthesis of multispectral bands from hyperspectral data: Validation based on images acquired by aviris, hyperion, ali, and etm+," *AVIRIS Workshop* (2002).
- [14] T., K., "Simulating landsat etm+ imagery using dais 7915 hyperspectral scanner data," *International journal of remote sensing* **25**(22), 5049–5067 (2004).
- [15] Baldrige, A. M., Hook, S. J., Grove, C. I., and g., R., "The aster spectral library version 2.0," *Remote Sensing of Environment* (2008).
- [16] Clark, R., Swayze, G., Wise, R., Livo, E., Hoefen, T., Kokaly, R., and Sutley, S., "Usgs digital spectral library splib06a," *U.S. Geological Survey, Digital Data Series 231* (2007).
- [17] Hueni, A., Nieke, J., Schopfer, J., Kneubler, M., and Itten, K., "The spectral database specchio for improved long-term usability and data sharing," *Computers & Geosciences* **35**, 557–565 (2009).
- [18] Ferwerda, J. G., Jones, S. D., and Reston, M., "A free online reference library for hyperspectral reflectance signatures," *SPIE Newsroom* (2006).
- [19] Davis, S. M. and Swain, P. H., [*Remote Sensing: The Quantitative Approach*], McGraw-Hill International Book Company (1978).
- [20] De Backer, S., Kempeneers, P., Debruyne, W., and Scheunders, P., "A band selection technique for spectral classification," *Geoscience and Remote Sensing Letters, IEEE* **2**(3), 319–323 (2005).
- [21] Mi-Hyun, P. and K., S. M., "Classifying environmentally significant urban land uses with satellite imagery," *Journal of environmental management* **86**(1), 181–192 (2008).
- [22] Riedmann, M. and Milton, E., "Supervised band selection for optimal use of data from airborne hyperspectral sensors," *IEEE Geoscience and Remote Sensing Symposium* **3**, 1770–1772 (2003).
- [23] Ranson, K. J., Kovacs, K., Sun, G., and Kharuk, V. I., "Disturbance recognition in the boreal forest using radar and landsat-7," *Canadian journal of remote sensing* **29**(2), 271–285 (2003).
- [24] Richards, J. A. and Jia, X., [*Remote Sensing Digital Image Analysis*], springer ed. (2006).
- [25] Kittler, J., Hatef, M., Duin, R. P. W., and Matas, J., "On combining classifiers," *IEEE Transaction on Pattern Analysis and Machine Intelligence* **20**(3), 226–239 (1998).